JOURNAL OF GEOPHYSICAL RESEARCH, VOL. 106, NO. C1, PAGES 1053–1065, JANUARY 15, 2001

Nitrous oxide cycling in the Arabian Sea

Hermann W. Bange, Spyridon Rapsomanikis,[1] and Meinrat O. Andreae

Biogeochemistry Department, Max Planck Institute for Chemistry, Mainz, Germany

Abstract. Depth profiles of dissolved nitrous oxide (N_2O) were measured in the central and western Arabian Sea during four cruises in May and July–August 1995 and May–July 1997 as part of the German contribution to the Arabian Sea Process Study of the Joint Global Ocean Flux Study. The vertical distribution of N_2O in the water column on a transect along 65°E showed a characteristic double-peak structure, indicating production of N_2O associated with steep oxygen gradients at the top and bottom of the oxygen minimum zone. We propose a general scheme consisting of four ocean compartments to explain the N_2O cycling as a result of nitrification and denitrification processes in the water column of the Arabian Sea. We observed a seasonal N_2O accumulation at 600–800 m near the shelf break in the western Arabian Sea. We propose that, in the western Arabian Sea, N_2O might also be formed during bacterial oxidation of organic matter by the reduction of IO_3^- to I^-, indicating that the biogeochemical cycling of N_2O in the Arabian Sea during the SW monsoon might be more complex than previously thought. A compilation of sources and sinks of N_2O in the Arabian Sea suggested that the N_2O budget is reasonably balanced.

1. Introduction

Nitrous oxide (N_2O) is an atmospheric trace gas that significantly influences, directly and indirectly, Earth's climate. In the troposphere it acts as a greenhouse gas and in the stratosphere it is the major source for NO radicals, which are involved in one of the main ozone reaction cycles [*Prather et al.*, 1996].

Recently published source estimates indicate that the world's oceans play a major, but not dominant, role in the global budget of atmospheric N_2O [*Bouwman et al.*, 1995; *Khalil and Rasmussen*, 1992]. Most of the world's ocean surface layer is near gas-exchange equilibrium with the atmosphere [*Nevison et al.*, 1995], whereas a subsurface N_2O accumulation is generally associated with the oxygen (O_2) minimum [e.g., *Butler et al.*, 1989; *Cohen and Gordon*, 1979; *Naqvi et al.*, 1994; *Oudot et al.*, 1990]. Significant N_2O depletion was observed in water masses showing intense denitrification, that is, anoxic basins [*Cohen*, 1978; *Elkins et al.*, 1978; *Hashimoto et al.*, 1983; *Rönner*, 1983] and oxygen depleted (suboxic) water bodies (for an overview see, *Codispoti et al.* [1992]). In most studies of oceanic N_2O, a positive linear correlation between excess N_2O (ΔN_2O = N_2O(observed) – N_2O(saturated)) and the apparent oxygen utilization (AOU = O_2(saturated) – O_2(observed)) was observed. This led to the prevailing view that during decomposition of organic material in the ocean, nitrification ($NH_4^+ \rightarrow NO_2^- \rightarrow NO_3^-$) is the main source for oceanic N_2O [*Butler et al.*, 1989; *Cohen and Gordon*, 1979; *Elkins et al.*, 1978; *Oudot et al.*, 1990; *Yoshinari*, 1976]. Based on recent dual-isotope measurements, *Dore et al* [1998] suggested that N_2O production via nitrification at the interface of the euphotic–aphotic zone plays an important role in the global tropospheric N_2O budget. However, from isotope measurements of the $\delta^{15}N$ and $\delta^{18}O$ values of N_2O in deep water, it is still under debate whether nitrification or denitrification ($NO_3^- \rightarrow NO_2^- \rightarrow N_2O \rightarrow N_2$) is the dominant production pathway in deep water [*Kim and Craig*, 1990; *Yoshida et al*, 1989]. At the boundaries of oxygen-depleted water bodies, both nitrification and denitrification or a coupling of both processes may produce N_2O [*Codispoti and Christensen*, 1985; *Law and Owens*, 1990; *Naqvi and Noronha*, 1991; *Naqvi et al.*, 1998; *Upstill-Goddard et al.*, 1999]. Here we present our measurements of nitrous oxide in the water column of the central and western Arabian Sea during the intermonsoon and southwest (SW) monsoon periods in 1995 and 1997.

2. Study Area and Sampling Locations

The northwestern part of the Indian Ocean is defined as the Arabian Sea (Figure 1). It is surrounded by the African and Asian continents to the west, north, and east. The southern boundary is usually set at the equator. The Arabian Sea experiences extremes in atmospheric forcing that lead to the greatest seasonal variability observed in any ocean basin. During the SW monsoon (late May to September), the strongest sustained wind stress is in the highly sheared Findlater Jet. The axis of the Findlater Jet extends generally from northern Somalia to northwestern India. During the SW monsoon, coastal upwelling is driven by Ekman divergence of surface water off shore owing to the influence of winds parallel to the coast. The region of coastal upwelling exists up to 400 km off the Arabian Peninsula. Downwelling occurs on the southeastern side of the Findlater Jet, driving subduction of surface waters into the thermocline and promoting deepening of the mixed layer.

The Arabian Sea contains diverse biogeochemical features such as eutrophic, oligotrophic, and low-oxygen environments. The latter lies between 150 and 1000 m depth and represents the thickest oxygen minimum zone (OMZ) found in the world's oceans today. The OMZ of the Arabian Sea is the site of intense denitrification processes and thus plays a major role in the global nitrogen cycle. For further details about the oceanographic and

[1] Now at Laboratory of Atmospheric Pollution Science and Technology, Environmental Engineering Department, Demokritos University of Thrace, Xanthi, Greece.

Paper number 1999JC000284
0148-0227/01/1999JC000284$09.00

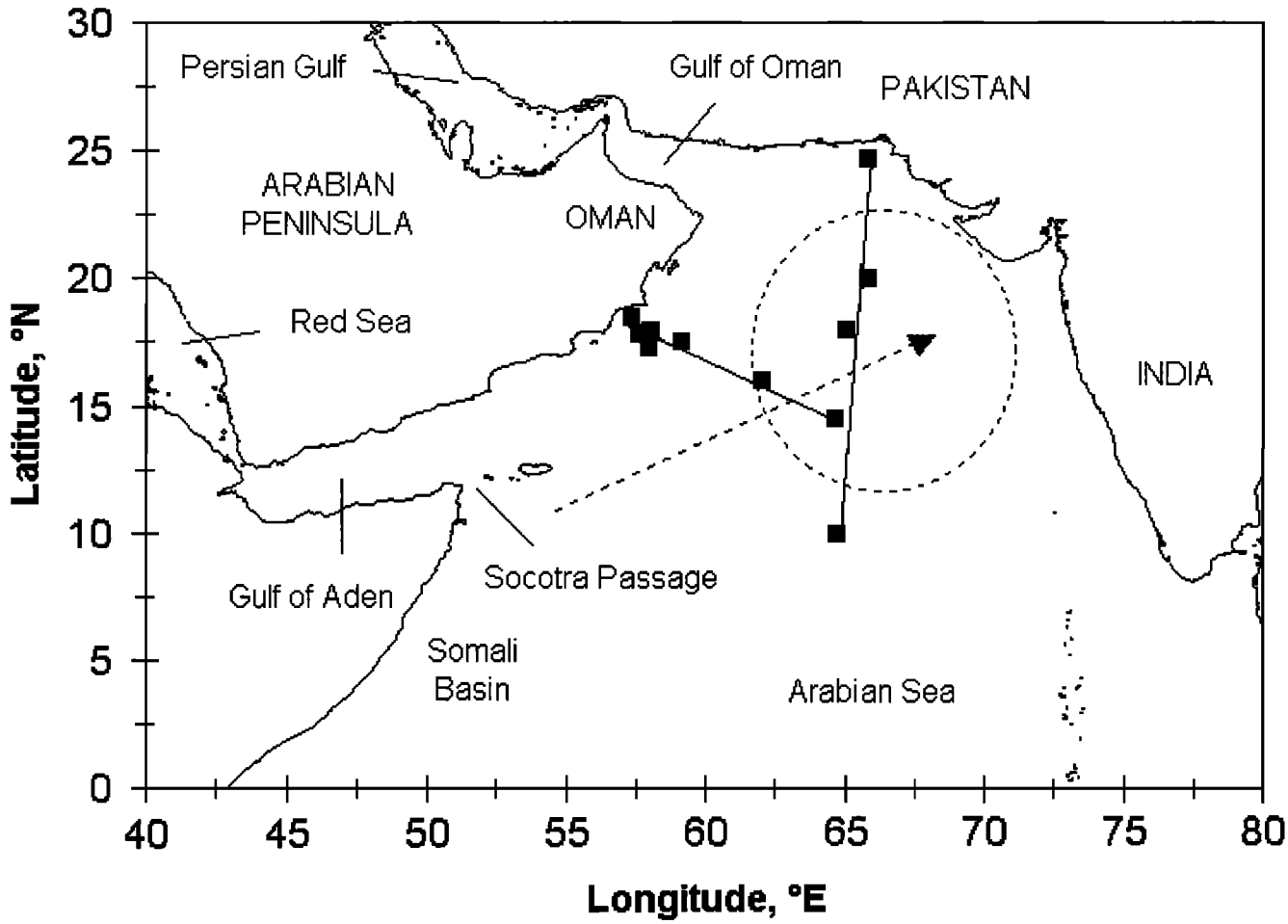

Figure 1. Map of the Arabian Sea with locations of selected stations where N_2O measurements were performed during the German JGOFS – Arabian Sea Process Study in 1995 and 1997 (for further details see Table 1). The two straight lines indicate the NS and NWSE transects as described in the text. The dashed arrow indicates the axis of the Findlater Jet. The dashed circle indicates the approximate distribution of the core of the denitrification zone as indicated by the secondary nitrite maximum ($NO_2^- > 1$ µmol L^{-1}) [*Naqvi*, 1994].

biogeochemical aspects of the Arabian Sea, the reader is referred to literature compilations presenting results from ongoing international research programs such as the Joint Global Ocean Flux Study (JGOFS) – Arabian Sea Process Study [*Burkill*, 1999; *Burkill et al.*, 1993; *Desai*, 1992; *Gage et al.*, 2000; *Ittekkot and Nair*, 1993; *Krishnaswami and Nair*, 1996; *Lal*, 1994; *Smith*, 1999, 1998; *Van Weering et al.*, 1997]. A comprehensive overview of the historical, geological, hydrographic, chemical, and biological aspects of the Arabian Sea in the context of the Indian Ocean is given in a recently published book by *Rao and Griffiths* [1998].

The four cruise legs discussed here were part of the German JGOFS – Arabian Sea Process Study and took place on the German research vessels *Meteor* (M) and *Sonne* (SO) in May 1995 (leg M32/3), July–August 1995 (leg M32/5), May–June 1997 (leg SO119), and June–July 1997 (leg SO120). Legs M32/3, M32/5, and SO119 covered mainly the central Arabian Sea, whereas leg SO120 focused on the coastal upwelling area off the Arabian Peninsula (Figure 1).

3. Method

Duplicate water samples from various depths were drawn into 100-mL glass flasks from bottles mounted on a rosette water sampler. Flasks with two outlets closed by Teflon valves and one outlet sealed with a silicone rubber septum for headspace sampling (Thermolite®, Restek GmbH, Germany) were used. The flasks were rinsed twice with at least two flask volumes of seawater prior to bubble-free filling with the seawater sample. Then 50 mL of the sample was replaced with helium and the remaining water phase was poisoned with saturated $HgCl_2$ solution (0.2 mL) [*Elkins*, 1980; *Yoshinari*, 1976]. Samples were stored at constant room temperature and allowed to equilibrate for at least 2 hours prior to chromatographic analysis. All samples were analyzed within 12 hours after collection. Prior to analysis, the samples were stirred with a magnetic stirrer for 5 min. A 10-mL subsample of the headspace was drawn with a gas-tight glass syringe from the flask and used to purge a thermostated (40°C), 2-mL sample loop connected to a 10-port gas stream selecting valve. Then the valve was switched and the sample was injected with the carrier gas onto the column. N_2O was determined using a gas chromatograph (Model 5890 Series II, Hewlett–Packard, California) equipped with an electron capture detector (ECD). The ECD (Model 19233, Hewlett–Packard, California) was held at a temperature of 350°C. The analysis was carried out at 190°C using a stainless steel column (1.83 m length, 3.2 mm OD, 2.2 mm ID) packed with washed molecular sieve 5A (mesh 80/100, Alltech GmbH, Germany). A mixture of Ar/CH_4

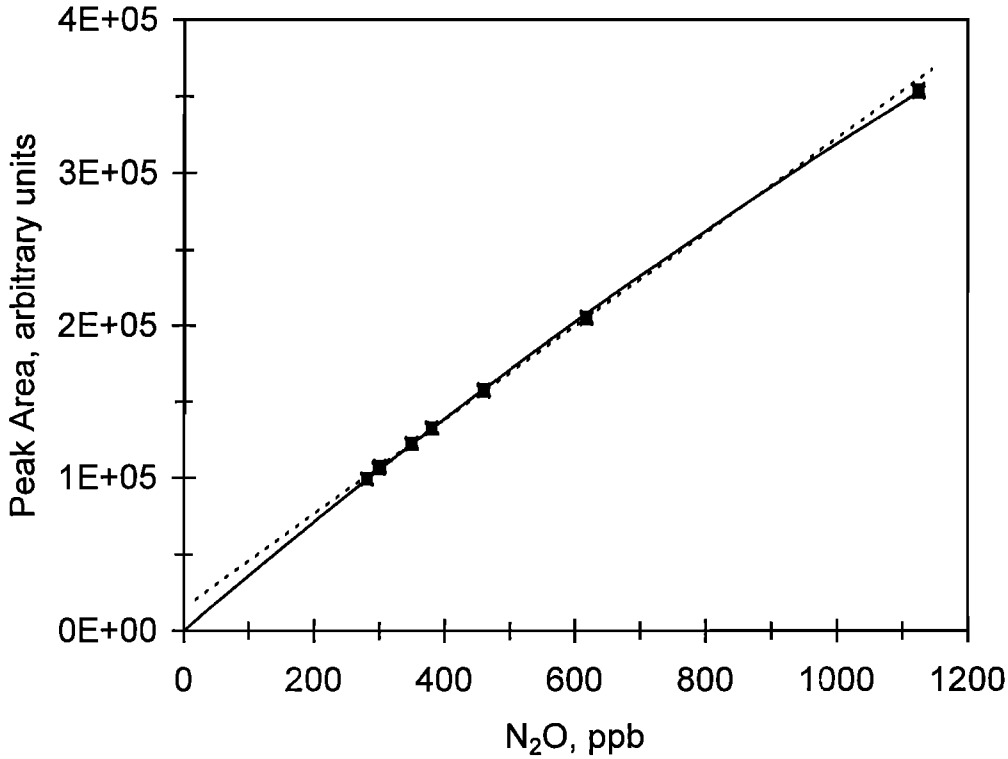

Figure 2. Characteristic response curve of the electron capture detector used in this study. We measured eight calibration gas mixtures: 299.0 ± 0.2, 300.5 ± 0.1, 349.6 ± 0.2, 380.5 ± 0.3 (all calibrated against the SIO-1993 standard scale (R. F. Weiss, personal communication, 1996), and 281, 460, 618, and 1125 ppb N_2O in synthetic air (± 2%; Deuste Steininger GmbH, Mühlhausen, Germany). The dashed line represents a linear fit through the points at 300.5 and 349.6 ppb N_2O (correlation coefficient r^2 = 0.9977, number of samples n = 19). The solid line indicates a quadratic fit ($y = -0.0458x^2 + 364.72x$, $r^2 = 0.9996$, number of samples $n = 47$). Read 4E+05 as 4×10^5.

(95%/5%) was used as the carrier gas at a flow rate of 45 mL min^{-1}. On a molecular sieve 5A column, CO_2 elutes after N_2O; the peaks are well separated under the conditions applied [*McAllister and Southerland*, 1971]. The use of the Ar/CH_4 mixture as carrier gas enhances the ECD sensitivity for N_2O and, additionally, avoids possible interferences from residual effects in the ECD owing to high CO_2 concentrations [*Butler and Elkins*, 1991].

Mixtures of N_2O in synthetic air were used to obtain two-point calibration curves. These mixtures contained 300.5 ± 0.1 and 349.6 ± 0.2 ppb N_2O, separately. These are gravimetrically prepared gas mixtures and were calibrated in the laboratory of R. F. Weiss (Scripps Institution of Oceanography (SIO), California), against the SIO-1993 standard scale (R. F.Weiss, personal communication, 1996). To account for the nonlinear ECD response [*Butler and Elkins*, 1991], we applied a quadratic regression ($y = ax^2 + bx$) for all values <300 ppb and a linear regression for values >300 ppb. Thus N_2O values in the range from 350 to 1050 ppb, which is above the range covered by the calibration gases, may be overestimated by as much as 2% owing to the linear regression applied (Figure 2). Concentrations of dissolved N_2O were calculated as follows:

$$[N_2O]_{dissolved} = [N_2O]_{water\ sample} + [N_2O]_{headspace}$$

$$= x'\beta(T, S)P + x'P/(RT)$$

and $x' = x/(P - p_{H2O})$, where x' is the N_2O dry mole fraction, β is the solubility function [*Weiss and Price*, 1980], T is the temperature of the sample at the time of the analysis, S is the salinity, P is the atmospheric pressure at the time of the analysis, R is the gas constant, x is the measured N_2O wet mole fraction in the headspace, and p_{H2O} is the water vapor pressure according to *Weiss and Price* [1980].

To check our method for systematic errors (e.g., efficiency of equilibration), we cross checked the values obtained by the method described above with the data from a well-established automated equilibration system for underway N_2O measurements in the surface layer. This system was run on board during the same cruises in 1995 and 1997 [*Bange et al.*, 1996, 2000]. The comparison shows a good agreement between both data sets (Figure 3), indicating that systematic errors are mainly introduced by the manual handling of the discrete samples. In order to calculate the theoretical overall analytical precision of our measurements, we assumed typical values and error ranges of 1±0.05 atm, 25±1°C, 35±0.1‰, and 100±10ppb for the pressure, equilibration temperature, salinity, and wet mole fraction, respectively. Computation of the error propagation gave an overall measurement error (i.e., $\Delta[N_2O]_{dissolved}$) of ±0.78 nmol L^{-1}. This results in a relative error ($\Delta[N_2O]_{dissolved}/[N_2O]_{dissolved}$) of ±12.4%. The computation of $\Delta[N_2O]_{dissolved}$ is most sensitive to errors in pressure, whereas errors of the equilibration temperature and salinity are less important. For example, an error of ±0.05 atm for the pressure results in an error of ±7.2%, whereas an error of ±1°C results in an error of ±1% for $\Delta[N_2O]_{dissolved}$. The precision of the measurements estimated from four replicate samples with an average concentration of 35.2 nmol L^{-1} was 7.7 %. This is in reasonable agreement with the theoretical overall error estimate given above.

Each N_2O depth profile is a composite of two casts covering different depth ranges collected at the same station within 24

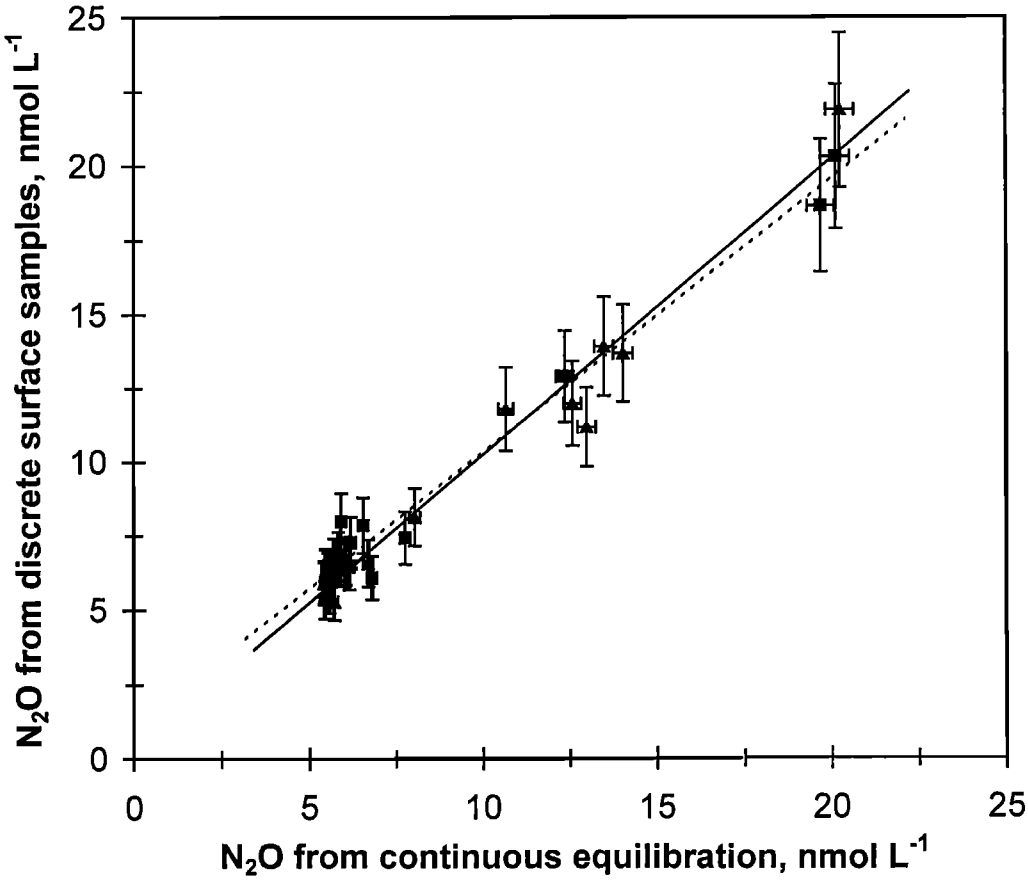

Figure 3. Comparison of N_2O surface concentrations measured by the discrete sampling method as described in the text (water depths 5–20 m) and a continuous equilibration system (pumping from 7 m water depth) [*Bange at al.*, 1996]. Solid squares represent data from M32/3 and M32/3. The dashed line is the linear regression for the data set from M32/3 and M32/5 ($y = 0.924x + 1.08$, $r^2 = 0.98$, $n = 12$). Solid triangles represent data from SO119 and SO120. The solid line is the linear regression for the data set from SO119 and SO120 ($y = 0.997x + 0.26$, $r^2 = 0.97$, $n = 16$).

hours. Equilibrium concentrations of dissolved N_2O and O_2 were calculated with the equations of *Weiss and Price* [1980] and *Weiss* [1970], respectively. We used an atmospheric N_2O dry mole fraction of 309 ppb [*Bange et al.*, 1996] and 311 ppb (H. W. Bange et al., unpublished data, 2000) for the calculation of the N_2O equilibrium concentrations in 1995 and 1997, respectively. Potential seawater temperatures were calculated with the equations listed in *Siedler and Peters* [1986]. Salinity, in situ water temperature, and nutrient data were taken from data compilations of measurements performed simultaneously to the water sampling (F. Pollehne et al., unpublished data, 1996; B. Zeitzschel et al., unpublished data, 1996, 1998; V. Ittekkot et al., unpublished data, 1998). All data presented are available from the German JGOFS Data Management Office (http://www.ifm.uni-kiel.de/pl/dataman/dmpag1.html).

4. Results and Discussion

Some selected stations (Table 1) were grouped into a north–south (NS) transect from 24.7°N to 10°N along 65°E during the intermonsoon period and into a northwest–southeast (NWSE) transect from 18.5°N, 56.5°E to 14.5°N, 65°E during the SW monsoon. (These transects are partly identical with the U.S. JGOFS standard cruise track in the Arabian Sea [*Smith*, 1998].) Depth profiles of the dissolved N_2O and O_2 along the NS and NWSE transects are shown in Figures 4 and 5, respectively.

4.1. NS Transect

The shapes of the N_2O profiles from the NS transect from the shelf break off Pakistan (24.7°N) to the central Arabian Sea (14.5°N) are clearly associated with the extremely low O_2 concentrations ($0 < O_2 < 20$ μmol L^{-1} or expressed in volumetric units $0 < O_2 < 0.25$ mL L^{-1}) in the OMZ in the Arabian Sea (Figures 4b–4d). These profiles have a characteristic double-peak structure. In the upper water column a marked increase in the N_2O concentrations from 5–6 nmol L^{-1} in the surface layer to about 25–55 nmol L^{-1} at 150 m depth forms the first sharp N_2O peak. This peak is followed by a pronounced depletion of dissolved N_2O at about 200–500 m water depth; even undersaturations with concentrations lower than 5 nmol L^{-1} were observed. This depletion of dissolved N_2O is most pronounced between 20° and 18°N (Figures 4c–4d). N_2O concentrations increase again up to 60 nmol L^{-1} at about 800 m to form the second N_2O peak (Figures 4c–4e), followed by a decrease with depth to values of 15 nmol L^{-1} in the deep and bottom waters. The profiles south of 10°N, which are outside the zone of extreme O_2 depletion in the OMZ as indicated by comparably higher O_2 concentrations (Figure 4f), generally showed a

Table 1. List of the Selected Stations Where N_2O Measurements Were Performed During the German JGOFS – Arabian Sea Process Study in 1995 and 1997[a]

Station	Position	Date	Cruise
	NS Transect		
EPT	27.7°N, 65.8°N	May 1997	SO119
NAST	20 0°N, 65 8°E	May 1997	SO119
D1[b]	18.0°N, 65 0°E	May 1995	M32/3
CAST	14 5°N, 65.0°E	May 1997	SO119
SAST/D2	10 0°N, 65.0°E	May 1997	SO119
	NWSE Transect		
CAST	14.5°N, 65 0°E	July 1995	M32/5
T2	16 0°N, 62.0°E	July 1997	SO120
T3	17.5°N, 59.1°E	July 1997	SO120
T4	18.1°N, 58.0°E	August 1995	M32/5
T5	17.3°N, 57.9°E	July 1997	SO120
T6	17.8°N, 57.6°E	July 1997	SO120
Shelf	18.5°N, 56.5°E	June 1997	SO120

[a] See also Figure 1.
[b] Measurements restricted for the depth range 0–2000 m. The profile is a composite of four casts from various depth ranges.

completely different shape of the profile. An accumulation of N_2O from the surface (up to 37 nmol L^{-1} between 500 and 1000 m) is followed by a decrease with depth (15 nmol L^{-1} in the deep and bottom waters) (Figure 4f).

Previous measurements of the depth distribution of N_2O in the Arabian Sea were performed in the central and western regions by *Law and Owens* [1990] (September–October 1986) and *Upstill-Goddard et al.* [1999], and in the central and eastern regions by *Naqvi and Noronha* [1991] (December 1988), *Lal et al.* [1996], and *Patra et al.* [1999] (April–May 1994, February–March 1995, July–August 1995). There is good agreement between the shapes of previously reported N_2O profiles and those presented in Figure 4. Both *Lal et al.* [1996] and *Naqvi and Noronha* [1991] also describe almost identical double-peak structures for stations in the northern central Arabian Sea (compare Figures 4b and 4c). However, there might be slight trends for the reported concentrations. Our maximum concentration along the NS transect was 58 nmol L^{-1} for the second N_2O peak at 18°N, 65°E (Figure 4d), whereas *Naqvi and Noronha* [1991] and *Patra et al.* [1999] observed concentrations up to 80 nmol L^{-1} for the second N_2O peak at 21.8°N, 64.6°E and 18°N, 67°E. *Law and Owens'* [1990] maximum N_2O concentration along their NS transect along 67°E was 59 nmol L^{-1} at 14.5°N, 66.9°E. Undersaturations in the core of the OMZ (compare Figures 3c and 3d) were also observed by *Law and Owens* [1990] and *Naqvi and Noronha* [1991] but not by *Patra et al.* [1999].

Comparison of the results from the various studies suggests that the distribution of N_2O in the central Arabian Sea is only partly known. Differences in the observed N_2O concentrations might result from the different spatial data coverage and/or temporal (i.e., seasonal and interannual) variability in the Arabian Sea (see also the discussion of the ΔN_2O–AOU relationships below). Profiles of N_2O typically show an accumulation in the OMZ of oceanic subsurface layers, most probably owing to nitrification [*Dore et al.*, 1998]. However, when extreme O_2 gradients at the boundaries of the OMZ exist, conditions become ideal for enhanced N_2O production by nitrification at low O_2 concentrations as well as for N_2O production by denitrification. Thus the first N_2O peak observed at approximately 150 m in the central Arabian Sea might result from a coupling of both [*Naqvi et al.*, 1998; *Naqvi and Noronha*, 1991]. Recent dual-isotope measurements indicate that denitrification might be the major production pathway for the second N_2O peak at the lower boundary of the OMZ in approximately 800–1000 m depth [*Naqvi et al.*, 1998]. The pronounced N_2O depletion in the core of the OMZ results from N_2O reduction to N_2 during intense denitrification at extremely low O_2 concentrations [*Naqvi and Noronha*, 1991]. Thus we conclude that the N_2O profiles at the NS transect reflect typical vertical distributions within (>10°N, Figures 4b–4e) and outside (<10°N, Figure 4f) the denitrification zone. Our results are in agreement with previously published ideas about the dominating N_2O production and consumption processes in the central Arabian Sea.

4.2. NWSE Transect

The distribution of dissolved N_2O on the NWSE transect appears to be more complex. The shape of the profile from station CAST (Figure 5b) indicates the characteristic double-peak shape for profiles from the northern part of the NS transect. Going further northwest to station T2 at 16°N, 62°E (Figure 5c), the typical upper N_2O peak at about 150–200 m was only weakly developed. However, following the transect further to the coast, the double-peak structure was again visible at stations T3, T4, and T5 (Figures 5d–5f). The N_2O profile at the shelf break off Oman (Figure 5g) is similar to the one observed at the shelf break off Pakistan (Figure 5f); however, the concentrations are higher at the coast off Oman. The highest concentrations (up to 64 nmol L^{-1}) during the German JGOFS cruises were observed at 700 m depth at station T4 (18°N, 58°E) (Figure 5e). Over the shelf with water depths of about 80 m, dissolved N_2O accumulates from 20 nmol L^{-1} in the surface layer to 40 nmol L^{-1} in the bottom layer (Figure 5h). The results of *Law and Owens* [1990] and *Upstill-Goddard et al.* [1999] also showed high N_2O concentrations (up to ΔN_2O of 104 nmol L^{-1} [*Law and Owens*, 1990]) in the western Arabian Sea, which are as high as those from the central Arabian Sea. Recently published N_2O profiles by *Upstill-Goddard et al.* [1999] from a similar NWSE transect, which was located north of the German JGOFS transect, are in general agreement with ours.

The temporal development of the distributions of N_2O and O_2 on the NWSE transect during three cruises in July–August 1995, May 1997 and June–July 1997 is shown in Plate 1. Using data from two different years may introduce a bias owing to a possible interannual variability; however, since we will focus on a qualitative rather than a quantitative interpretation our approach might be reasonable. The O_2 depleted layer (<20 μmol L^{-1}) extends to the shelf of the Arabian Peninsula, showing only a modest temporal variation (Plates 1d–1f). In contrast, the N_2O concentrations show a considerable seasonal signal (Plates 1a–1c). While during May 1997 (Plate 1a), an N_2O plume originating from the central Arabian Sea is visible, the situation during the early stage of the SW Monsoon (June–July 1997, Plate 1b) and during the fully developed SW Monsoon (July–August 1995, Plate 1c) is completely different. During the SW Monsoon the development of a strong local source of N_2O near the shelf break at 700 m depth (corresponding to a potential density (σ_θ) of 27.3) is obvious. Either an in situ source (e.g., denitrification) or a seasonally occurring boundary current transporting N_2O-enriched water might be the reason for the observed enhanced N_2O concentrations:

1. Water mass analysis indicated that Red Sea water with a

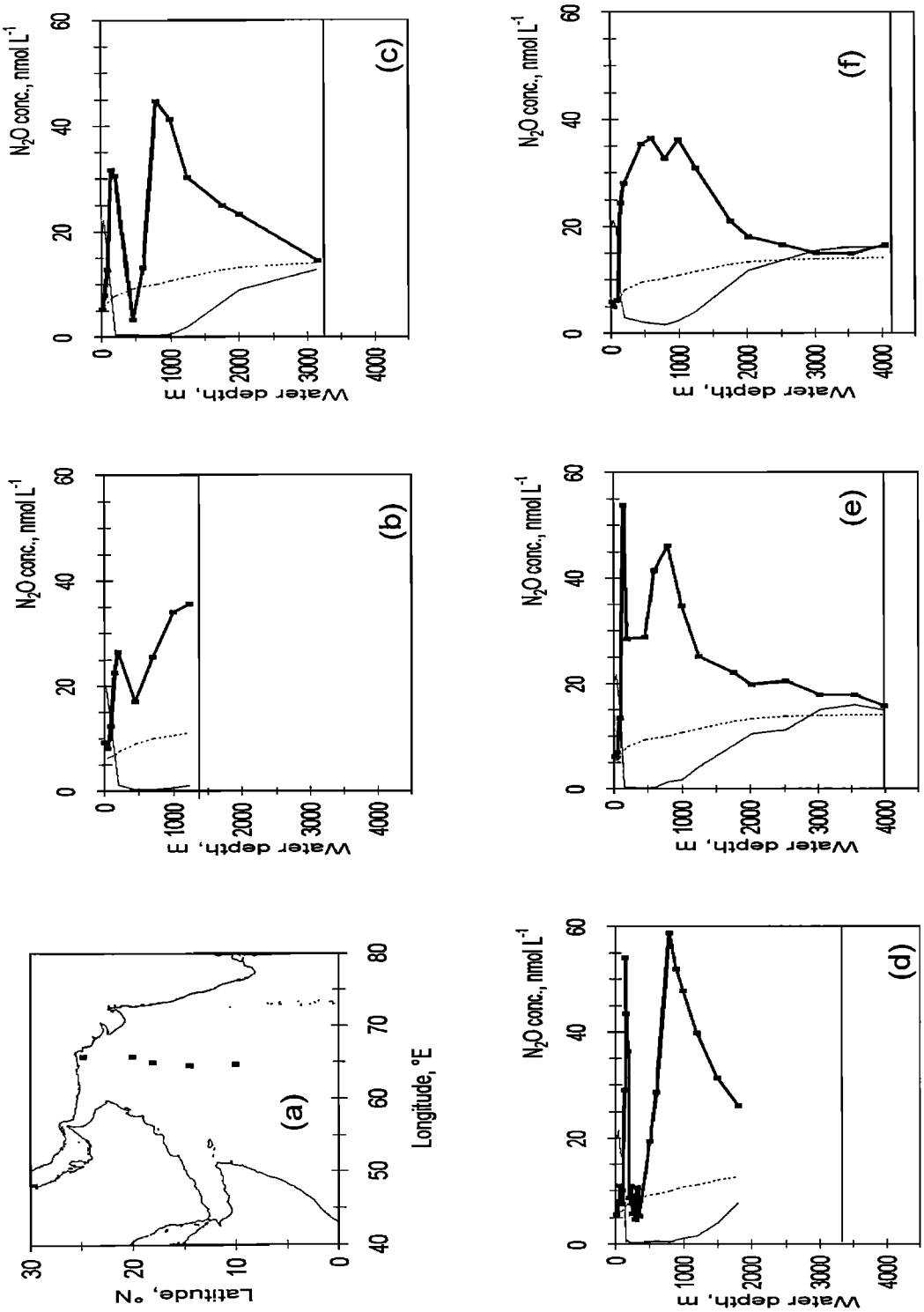

Figure 4. Concentrations of N_2O (in nmol L^{-1}) and O_2 (in 10^{-1} µmol L^{-1}) along the NS transect along 65°E (thick line, dissolved N_2O; dashed line, calculated equilibrium N_2O; thin line, O_2 concentration ; the horizontal line indicates sea bottom). (a) Map with station locations, (b) EPT, (c) NAST, (d) D1, (e) CAST, and (f) SAST. For an overview of the station positions and dates of measurements, see Table 1.

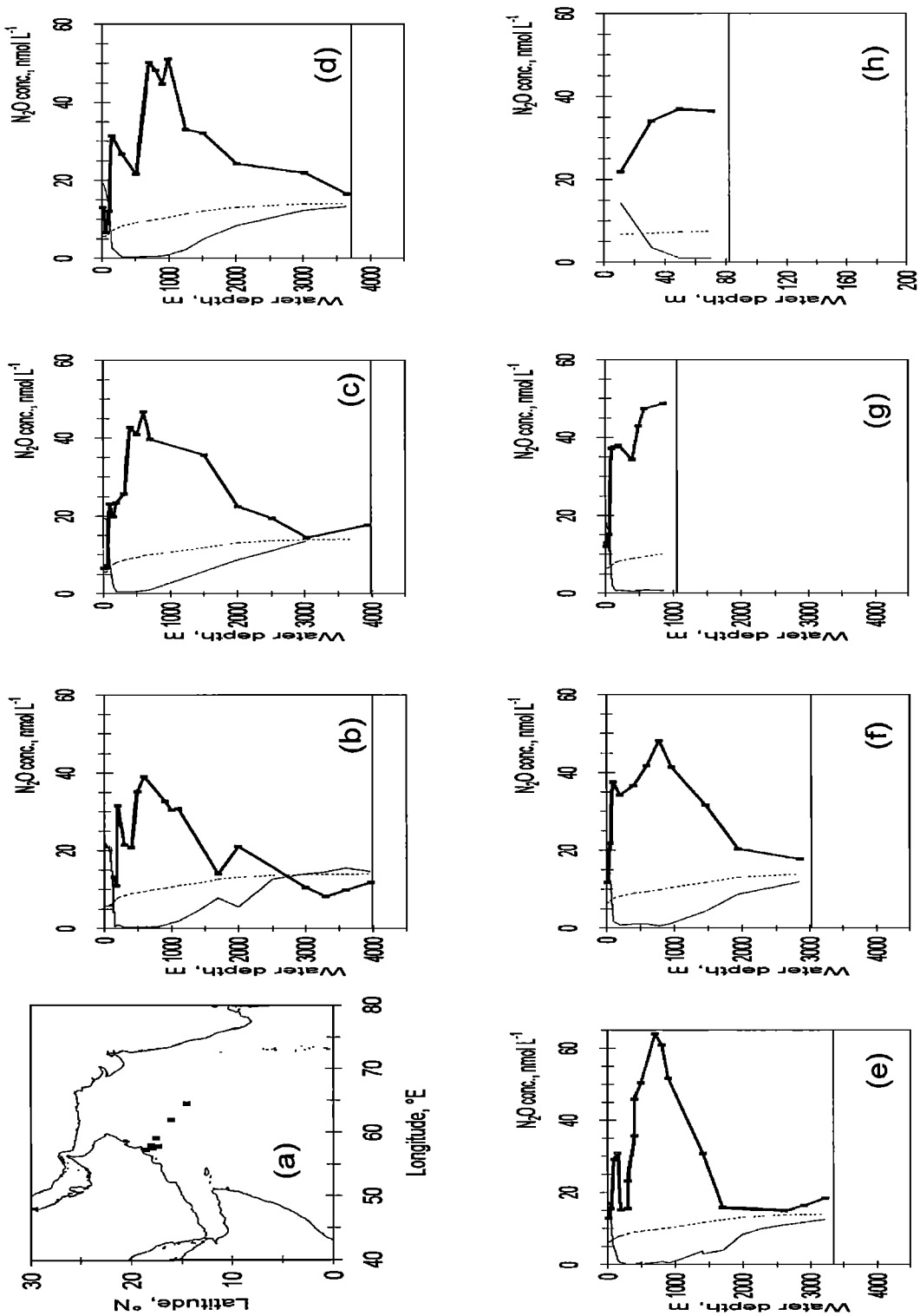

Figure 5. Concentrations of N_2O (in nmol L^{-1}) and O_2 (in 10^{-1} µmol L^{-1}) along the NWSE transect (thick line, dissolved N_2O; dashed line, calculated equilibrium N_2O; thin line, O_2 concentration; horizontal line indicates sea bottom). (a) Map with station locations, (b) CAST, (c) T2, (d) T3, (e) T4, (f) T5, (g) T6, and (h) shelf. For an overview of the station positions and dates of measurements, see Table 1.

core σ_θ of 27.2 at 600–700 m was not detectable, probably because its inflow to the Arabian Sea is usually blocked during the SW Monsoon [*Morrison et al.*, 1998; *Shenoi et al*, 1993]. Instead, we can speculate that an inflow of N_2O-enriched water from the Somali Basin [*De Wilde and Helder*, 1997] through the Socotra Passage might occur [*Schott et al.*, 1997; *You*, 1997].

2. The O_2 concentrations in the OMZ on the NWSE transect were depleted in O_2, comparable to those in the central Arabian Sea and favoring conditions for denitrification. However, the OMZ of the western Arabian Sea is not characterized by the permanent secondary nitrite (NO_2^-) maximum [*Morrison et al.*, 1998], which is often used as an indicator for the occurrence of denitrification [*Naqvi*, 1991].

Interestingly, *Farrenkopf et al.* [1997] found extremely high subsurface maxima of iodide (I^-) near the Arabian Peninsula (around 17°N, 57°E) at 600–800 m depth (σ_θ = 27.3–27.5). They concluded that, within the OMZ, organic matter decomposition via bacterial reduction of iodate (IO_3^-) to I^- could be as important as denitrification. A possible decomposition of organic matter via oxidation by IO_3^- to yield N_2O might be written as follows:

$$81.3\ IO_3^- + (CH_2O)_{106}(NH_3)_{16}H_3PO_4$$

$$\rightarrow 81.3\ I^- + 106\ CO_2 + 8\ N_2O + 130\ H_2O + H_3PO_4.$$

Following the concept of *Froelich et al.* [1979] ($\Delta G°$ data were taken from *Stumm and Morgan* [1996]), we calculated for the reaction given above a $\Delta G° = -2712$ kJ per mole glucose, which is comparable with $\Delta G°$ values given for the oxidation of organic matter by IO_3^- yielding NH_3 (–2605 kJ mol^{-1}), HNO_3 (–2804 kJ mol^{-1}), or N_2 (–3047 kJ mol^{-1}) [*Farrenkopf et al.*, 1997]. Despite the fact that the I^- data from *Farrenkopf et al.* [1997] are from the transition from the SW monsoon to the intermonsoon (October 1992) and might be therefore not representative for the peak of SW monsoon (July–August), we speculate that the observed enhanced N_2O concentrations might be coupled to a bacterially mediated IO_3^-/I^- cycle. The mean decomposition of particulate organic matter between 505 and 809 m water depth at U.S. JGOFS station S2 (18.1°N, 58°E) measured during the spring intermonsoon and SW monsoon 1995 was about 1.5 μmol C m^3 d^{-1} [*Lee et al.*, 1998]. Converting this with the molar ratio of N_2O to organic carbon of 8/106 (see equation above) yields a theoretical N_2O production of 0.113 μmol m^3 d^{-1}. From our measurements we estimated an accumulation of N_2O between 500 and 800 m of about 20 nmol L^{-1} from May to August (Plates 1a–1c). Assuming that this accumulation is representative for the time interval of the organic flux measurements (204 days), we estimated the N_2O production to be about 0.098 μmol m^3 d^{-1}. Thus the observed N_2O accumulation is slightly lower than the theoretically predicted N_2O production, indicating that the decomposition of organic carbon via the IO_3^-/I^- mechanism might contribute to the N_2O production. However, it is very unlikely that almost all organic carbon is converted to N_2O. More likely a mixture of N_2O and more energetically favored products (e.g., N_2) will occur. We conclude that there is not yet a satisfactory explanation for the local source of N_2O at the shelf break in the western Arabian Sea; neither an inflow event nor enhanced N_2O production via denitrification or other mechanisms have been substantiated.

4.3. ΔN_2O–AOU Relationship

As mentioned in the introduction, a positive correlation between ΔN_2O and AOU, indicating N_2O formation via

Table 2. ΔN_2O–AOU ($\Delta N_2O = m\text{AOU} + n\text{AOU}^2 + b$) Relationships for the Arabian Sea[a]

Arabian Sea Region	Date	*m*, *n*	*b*	r^2 / Number of Samples	Remarks	References
Central/west	Sept.–Oct. 1986	0 033, 0	5 5	(both significant at the 1% level)	AOU <197	*Law and Owens* [1990]
		0.310, 0	–49.4		AOU >197	
Central/east	Dec. 1988	(0.1066 + 0.00455 *t*), 0	3.2	not given	O_2 > 0.25 mL L^{-1}, *t* is temperature in °C	*Naqvi and Noronha* [1991]
Somali Basin, Gulf of Aden	July–Aug. 1992	0.172, 0	–1.26	0 92 / 51	intermediate waters <2000 m	*De Wilde and Helder* [1997]
Central/east	April–May 1994	0.1482, 0	1 03	0.71 / 31	water depths <1000 m and 0<AOU<200	*Patra et al.* [1999]
	Feb.–March 1995	0.1553, 0	3 05	0.65 / 59		
	July–Aug 1995	0.1464, 0	1 17	0.90 / 30		
Central/west	Aug.–Oct. 1994	0.049[b], 0.0004	0.83	not given	water depth <500 m	*Upstill-Goddard et al* [1999]
		–1 58, 0.0043	151.3		water depth >500 m	
	Nov.–Dec. 1994	0.007[b], 0.0006	0.25		only valid above OMZ	
Central/west	May 1995	0.1256, 0	1.31	0.81 / 16	water depth <150 m	this study
	July–Aug. 1995	0.0935, 0	2.12	0 73 / 41		
	May 1997	0.0799, 0	2.71	0.66 / 33		
	June–July 1997	0.1056, 0	1.84	0.86 / 45		
Central/west	May 1995	0.0952, 0	2 00	0.70 / 46	water depth <2000 m and O_2>0.25 mL L^{-1}	this study
	July–Aug 1995	0.0609, 0	1.61	0 48 / 39		
	May 1997	0.0700, 0	2.55	0.63 / 63		
	June–July 1997	0.0865, 0	3.27	0.70 / 51		
Central/west	July–Aug 1995	0.0910, 0	–15.0	0.14 / 46	water depth >2000 m	this study
	May 1997	0.0672, 0	–11.0	0.25 / 15		
	June–July 1997	0.3363, 0	–68.4	0.55 / 5		

[a] ΔN_2O in nmol L^{-1} and AOU in μmol L^{-1}. *r* stands for correlation coefficient.
[b] Original values (–0.049, –0 007) were reported erroneously (R. C. Upstill-Goddard, personal communication, 2000).

Table 3. Rates of N_2O Production in the OMZ ($O_2 < 0.25$ mL L^{-1}) of the Central Arabian Sea

	Integrated ΔN_2O,[a] Tg N_2O	Range of N_2O Production Using 1- / 10-Year Ventilation Time,[b] Tg N_2O yr^{-1}
May 1995	2.5	2.5 / 0.25
July–Aug. 1995	1.9 ± 0.5	1.9 / 0 19
May 1997	1.6 ± 0 3	1.6 / 0.16
June–July 1997	2 4 ± 0.5	2.4 / 0 24
Average	2.1	2.1 / 0.21

[a] Calculated as mean vertical integrated ΔN_2O times area of the OMZ affected by denitrification (1.95 x 10^{12} m^2, [*Naqvi*, 1991]).
[b] One-year ventilation time according to *Naqvi and Shailaja* [1993]; 10-year ventilation time according to *Olson et al* [1993].

nitrification, is found in a variety of oceanic environments. An overview of previously published ΔN_2O–AOU relationships for the Arabian Sea together with those calculated on the basis of our N_2O data is presented in Table 2. In a recent study, *Upstill-Goddard et al* [1999] showed that a second-order polynomial gave the best statistical fit to their data from the western and central Arabian Sea. We found considerable differences between the various ΔN_2O–AOU relationships. Even for data from the same year and season (e.g., July–August 1995, Table 2), the values differ considerably and could be explained only by a different spatial data coverage. Seasonal or interannual trends might be obscured in the data for various reasons, such as the difference in the yield of N_2O production owing to the composition and the amount of organic matter to be oxidized or to an additional N_2O source, e.g., assimilatory nitrate reduction [*Elkins et al.*, 1978]. Assimilatory nitrate reduction ($NO_3^- \rightarrow NO_2^- \rightarrow NH_4^+$) was proposed by some authors as a possible source of N_2O in nitrate-enriched waters, e.g., in upwelling regions; however, this hypothesis has never been proved [*Oudot et al.*, 1990; *Pierotti and Rasmussen*, 1980]. Most ΔN_2O–AOU relationships for the Arabian Sea are based on data sets excluding data affected by denitrification in the OMZ (i.e., $O_2 < 0.25$ mL L^{-1}). This indicates a shift in the pathways of N_2O production from nitrification to denitrification in the OMZ of the central Arabian Sea, which can not be represented by the common ΔN_2O–AOU relationship. The situation is even more complicated because N_2O can also be consumed during denitrification, leading to low N_2O values in the core of the OMZ in the central Arabian Sea. Despite the fact that the ΔN_2O–AOU relationships for deep water (>2000 m) are statistically not significant, they all show similar positive trends comparable to those observed for the upper ocean (Table 2). Thus we can speculate that nitrification is still the main pathway for N_2O production, but it might be balanced by subsequent N_2O reduction via denitrification as proposed by *Kim and Craig* [1990].

4.4. N_2O Budget for the Arabian Sea

To obtain knowledge of the N_2O production in the Arabian Sea, we estimated N_2O production for the OMZ affected by denitrification ($O_2 < 0.25$ mL L^{-1}) (Table 3). For this purpose we calculated the N_2O column abundances, defined as the vertically integrated profile of ΔN_2O. With the mean ΔN_2O calculated for each leg, it is possible to estimate the net N_2O production within the OMZ, assuming an area for the denitrification of 1.95 x 10^{12} m^2 [*Naqvi*, 1991] and a ventilation time of 1–10 years [*Naqvi and Shailaja*, 1993; *Olson et al.*, 1993]. The applied OMZ area affected by denitrification is 30% higher than the revised value of 1.37 x 10^{12} m^2 recently proposed by *Naqvi* [1991]. However, using a larger area appears more appropriate to account for the area distribution of the N_2O production processes (see discussion of the NWSE transect above). Moreover, the considerable range in the OMZ ventilation times (1–11 years) reported in the literature (for a discussion see *Naqvi* [1994]) introduces a more significant uncertainty.

Annual N_2O production in the OMZ was previously calculated to be 0.4 Tg by *Mantoura et al.* [1993] on the basis of the 1986 data set of *Law and Owens* [1990]. However, *Mantoura et al.* [1993] used a 10-year ventilation time; thus their value can be considered as a lower limit. Applying a ventilation time of 1 year scales their value up to 4 Tg N_2O yr^{-1}. A comparison with our results (0.2–2 Tg N_2O yr^{-1}, Table 3) reveals that the results are in reasonable agreement, despite possible biases due to seasonal and interannual variabilities. We calculated a mean N_2O production in the OMZ of 1.1 Tg yr^{-1} (i.e., 0.7 Tg N yr^{-1}) which represents about 2% of the mean pelagic denitrification of about 33 Tg N yr^{-1} [*Bange et al.*, 2000].

Table 4. N_2O Budget for the Arabian Sea North of 6°N

	Mean, Tg N_2O yr^{-1}	Range, Tg N_2O yr^{-1}	References
	Sources		
Net N_2O production in the OMZ	1.7	0.2–2	this study, Table 3
		0.4–4[a]	*Mantoura et al* [1993]
N_2O input by Red Sea and Persian Gulf	0.03[b]	0–0.06[c]	
N_2O input across 6°N	0.1	0–0 2[c]	this study, Figure 6
	Sinks		
Loss to the atmosphere	0.4	0.2–0.6	*Bange et al.* [2000]
Loss in eastern margin sediments	1.3	not given	*Naqvi and Noronha* [1991]
Sources – sinks	0.13		

[a] Original value of 0.25 Tg N yr^{-1} (0.4 Tg N_2O yr^{-1}) scaled to an OMZ ventilation time of 3 years.
[b] *Rhein et al.* [1997] estimated inflows of 0 3 x 10^6 m^3 s^{-1} for Red Sea (σ_θ = 27 2) and 0.18 x 10^6 m^3 s^{-1} for the Persian Gulf (σ_θ = 26.6) waters. Associated N_2O concentrations were 60 nmol L^{-1}, estimated from *De Wilde and Helder's* [1997] station 276-04 (400–700 m) in the Gulf of Aden in August 1992, and 21 nmol L^{-1} calculated from *Law and Owens'* [1990] northernmost station (station 11, 24.8°N, 57 2°E, September 1986) in the Gulf of Oman.
[c] We assumed an error of ±100% owing to the implicit considerable uncertainties of our estimate.

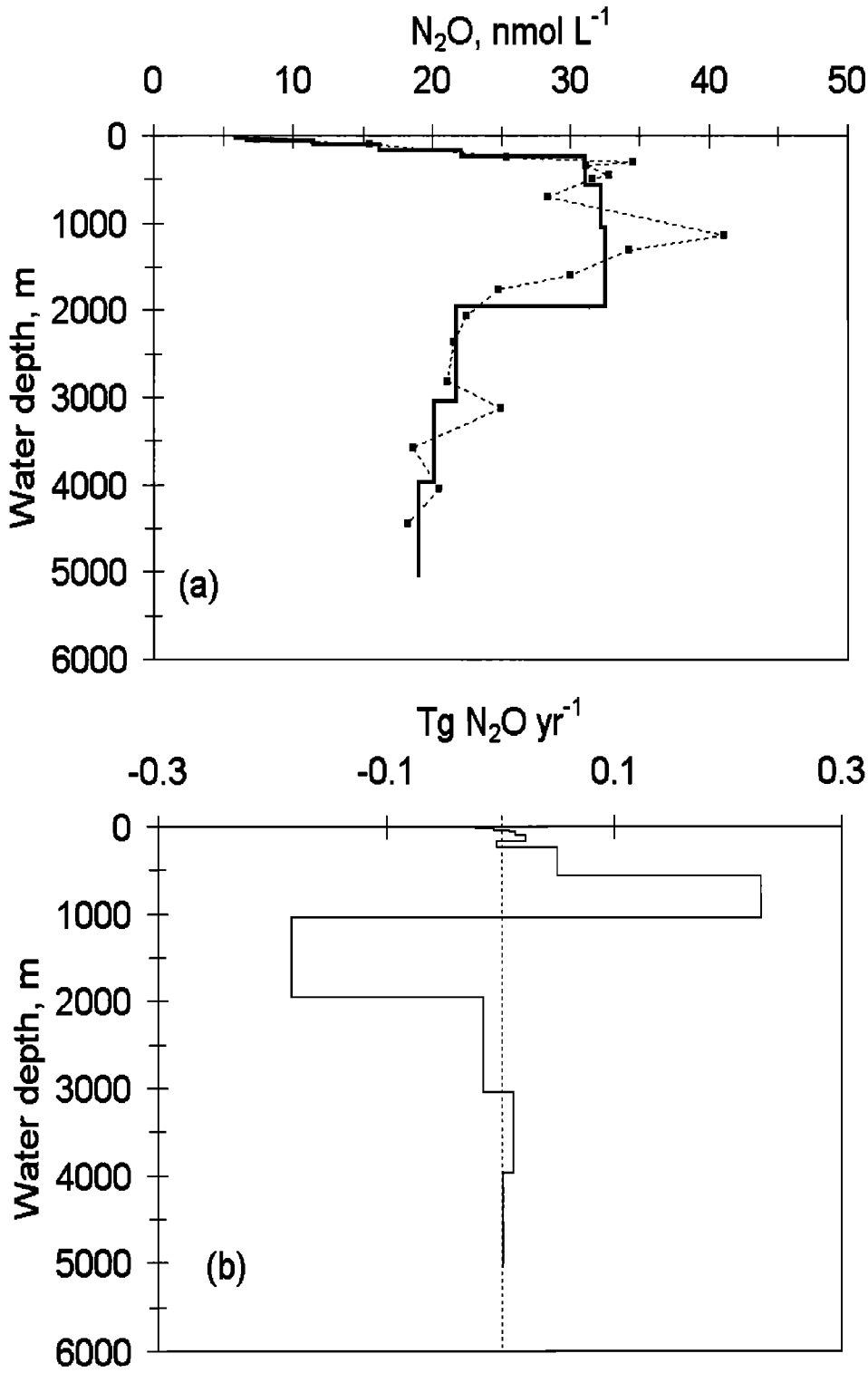

Figure 6. N_2O flux into and out of the Arabian Sea along 6°N: (a) N_2O concentrations (dashed line, N_2O profile at 6°N, 65°E in July 1995 during cruise M32/5; solid line, calculated standard level mean N_2O profile). (b) Resulting mean annual N_2O flux for the layers of the GCM (negative values represent outflows and positive values represent inflows into the Arabian Sea across 6°N).

An overall N_2O budget for the Arabian Sea based on the data presented here and found in the literature is presented in Table 4. In order to obtain consistent N_2O flux estimates we adopted the approach used by *Bange et al.* [2000] for a revision of the nitrogen fluxes of the Arabian Sea. The southern boundary of the Arabian Sea was set to 6°N spanning a line from the Somali coast to the southern tip of Sri Lanka (for details see *Bange et al.* [2000]).

In order to assess the mean annual N_2O exchange across the southern boundary of the Arabian Sea at 6°N, monthly values for

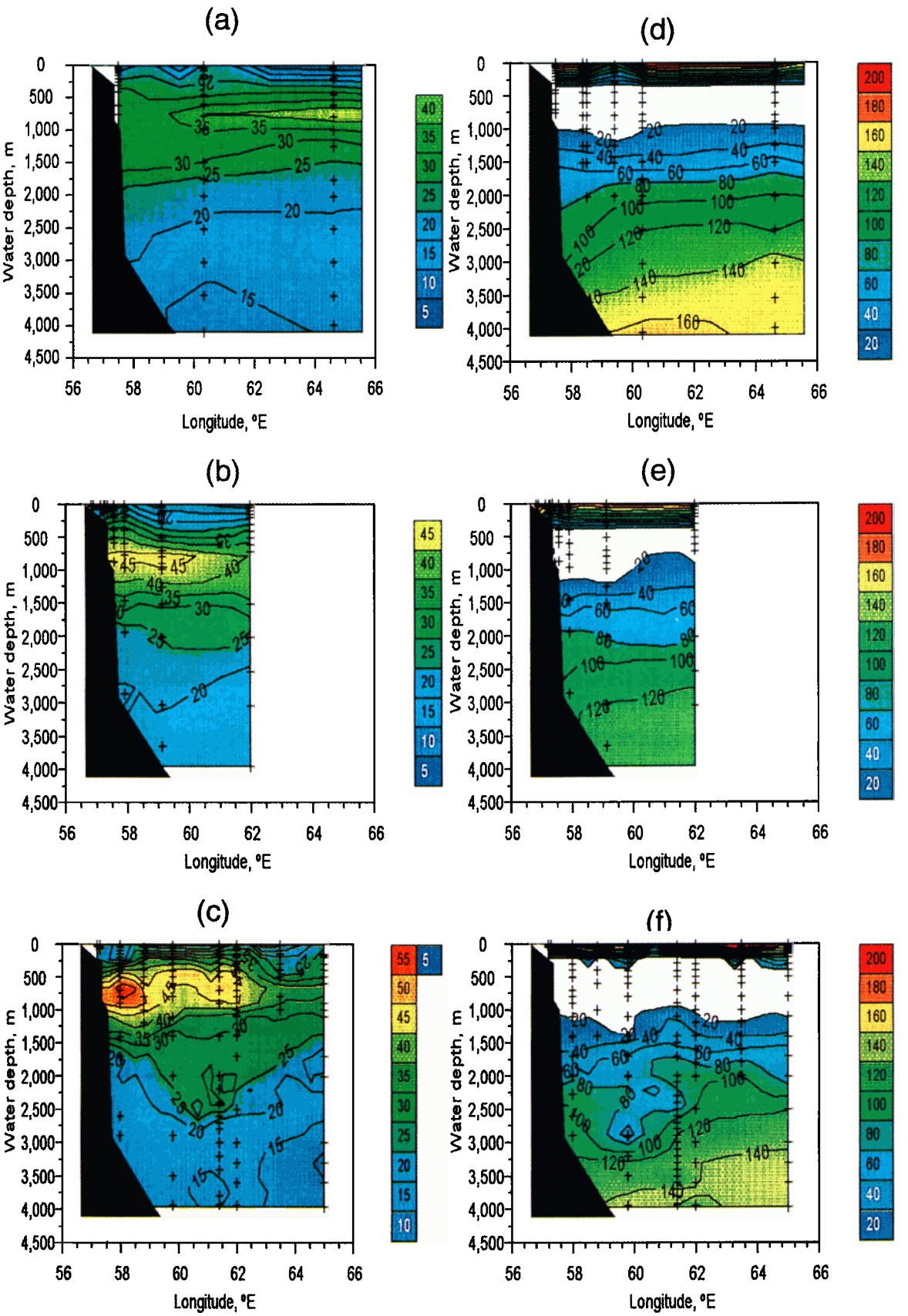

Plate 1. Concentrations of N_2O (in nmol L^{-1}) and O_2 (in μmol L^{-1}) along the NWSE transect in the western Arabian Sea. (left), N_2O: (a) May 1997, (b) June–July 1997, and (c) July–August 1995. (right), O_2 (white areas indicate concentrations below 20 μmol L^{-1}): (d) May 1997, (e) June–July 1997, and (f) July–August 1995.

the water transport across 6°N were extracted from a general circulation model (GCM) consisting of 13 depth layers with a 1° x 1° horizontal resolution (for details see *Bange et al.* [2000]). N_2O values were taken from a profile at 6°N, 65°E (July 1995, M32/5). The N_2O concentrations were scaled to the grid points of the GCM (Figure 6a). Then we calculated for each grid point the mean annual N_2O flux. Summing the fluxes yields the net N_2O fluxes for each layer (Figure 6b). The resulting overall net flux sums up to an annual input into the Arabian Sea of about 0.1 Tg N_2O. The major sink for N_2O in the Arabian Sea is its consumption in eastern margin sediments and the major source is the N_2O production in the OMZ. Inputs by Red Sea and Persian Gulf waters as well as advective input from the south appear to play only a minor role. The budget from the data in Table 4 seems to be reasonably balanced. However, the magnitude of the sedimentary N_2O loss is under debate. As discussed by *Naqvi et al.* [1992], the observed N_2O gradients at the eastern margin sediments could also result from advective processes, indicating an overestimation of the N_2O sink in the sediments. Moreover, our estimate of the N_2O emissions to the atmosphere might be too low since recent N_2O measurements in the upwelling region off southwestern India during the SW monsoon showed extremely high N_2O concentrations [*Naqvi et al*, 1998], which may lead to an upward revision of the current N_2O emission estimates.

5. Conclusions

A compilation of sources and sinks of N_2O in the Arabian Sea suggested that the N_2O budget is reasonably balanced. In view of our results, we propose a rough scheme of N_2O production and consumption pathways in the Arabian Sea. Our scheme consists of four compartments that could explain the characteristic double-peak structure of N_2O in the Arabian Sea:

Compartment 1, 0–150 m: N_2O is mainly produced by nitrification as indicated by the ΔN_2O–AOU relationships (Table 2). However, isotope data measured by *Naqvi et al.* [1998] revealed that nitrification may not be the only source. N_2O may also be produced via coupling of nitrification and denitrification associated with the steep O_2 gradient at the top of the OMZ, forming the sharp N_2O peak at about 150 m [*Naqvi et al.*, 1998].

Compartment 2, 150–1000 m: N_2O consumption occurs at 300–500 m (i.e., the denitrifying core of the OMZ) of the central Arabian Sea. At the lower boundary of the OMZ at about 800–1000 m, N_2O seems to be mainly produced by denitrification when the O_2 concentrations are increasing again [*Naqvi et al.*, 1998].

Compartment 3, 1000–2000 m: In the central Arabian Sea the denitrification signal (i.e., $\delta^{15}N$ of NO_3^-) is assumed to be mixed down to a depth of at least 1500 m owing to ventilation processes such as cross-isopycnal mixing [*Brandes et al.*, 1998]. This implies that N_2O produced at the bottom of the OMZ is also mixed down by cross-isopycnal mixing, forming the broad second N_2O peak. ΔN_2O–AOU relationships (excluding data affected by denitrification) are reasonably valid from 0–2000 m (Table 2) Thus we can conclude that nitrification contributes significantly to the N_2O production throughout the water column; however, the N_2O produced by denitrification results in less clear ΔN_2O–AOU relationships.

Compartment 4, below 2000 m: No statistically significant ΔN_2O–AOU relationship was found. N_2O produced by nitrification may be reduced subsequently by denitrification [*Kim and Craig*, 1990].

This scheme may also be valid for the western Arabian Sea; however, owing to the seasonal variability of the complex hydrographic situation (e.g., coastal upwelling, inflow of marginal sea water), the N_2O double-peak structure is not well-established. Furthermore, we have some indication that N_2O at 600–800 m near the shelf break in the western Arabian Sea is formed via a different process such as oxidation of organic matter by reduction of IO_3^- to I^-, indicating that the biogeochemical cycling of N_2O in the central and western Arabian Sea during the SW Monsoon is more complex than previously thought.

Acknowledgments. We thank G. Schebeske and our glass blower B. Beickler for their invaluable assistance. We acknowledge the help of many other colleagues and the officers and crews of the R/V *Meteor* and R/V *Sonne*. Thanks are due to the chief scientists F. Pollehne (M32/3), B. Zeitzschel (M32/5 and SO120), and V. Ittekkot (SO119) Special thanks are due to the team of the R/V *Sonne* scientific-technical service for their support on board. We are indebted to many colleagues for their generosity in sharing data. We especially thank C S Law for providing his N_2O data from the 1986 Arabian Sea expedition We thank C. Strametz for help with the manuscript. We gratefully acknowledge J M. Lobert and two anonymous reviewers for their constructive criticisms of the manuscript. The investigations were financially supported by the German Bundesministerium für Bildung, Wissenschaft, Forschung und Technologie through grants 03F0137A, 03F0183G, 03F0241C and by the Max Planck Society.

References

Bange, H.W., S. Rapsomanikis, and M O Andreae, Nitrous oxide emissions from the Arabian Sea, *Geophys. Res Lett.*, *23*, 3175–3178, 1996.

Bange, H.W., T Rixen, A.M. Johansen, R L. Siefert, R Ramesh, V. Ittekkot, M R. Hoffmann, and M.O Andreae, A revised nitrogen budget for the Arabian Sea, *Global Biogeochem. Cycles*, in press, 2000.

Bouwman, A F , K W Van der Hoek, and J.G J Olivier, Uncertainties in the global source distribution of nitrous oxide, *J. Geophys. Res*, *100*, 2785–2800, 1995.

Brandes, J.A , A.H. Devol, T Yoshinari, D.A Jayakumar, and S.W.A. Naqvi, Isotopic composition of nitrate in the central Arabian Sea and eastern tropical North Pacific. A tracer for mixing and nitrogen cycles, *Limnol. Oceanogr.*, *43*, 1680–1689, 1998.

Burkill, P.H (Ed.), Arabesque, UK JGOFS Process Study of the Arabian Sea, *Deep Sea Res , Part II, 46*, 529–863, 1999.

Burkill, P H., R.F.C. Mantoura, and N.J.P. Owens (Eds.), Biogeochemical cycling in the northwestern Indian Ocean, *Deep Sea Res , Part II, 40*, 643–849, 1993.

Butler, J.H , and J.W. Elkins, An automated technique for the measurements of dissolved N_2O in natural waters, *Mar. Chem.*, *34*, 47–61, 1991.

Butler, J H , J W. Elkins, T.M. Thompson, and K.B. Egan, Tropospheric and dissolved N_2O of the West Pacific and Indian Oceans during the El Niño Southern Oscillation event of 1987, *J Geophys. Res.*, *94*, 14,865–14,877, 1989.

Codispoti, L.A., and J.P. Christensen, Nitrification, denitrification and nitrous oxide cycling in the Eastern Tropical South Pacific, *Mar. Chem , 16*, 277–300, 1985.

Codispoti, L.A., J.W. Elkins, T. Yoshinari, G.E. Friederich, C.M. Sakamoto, and T T. Packard, On the nitrous oxide flux from productive regions that contain low oxygen waters, in *Oceanography of the Indian Ocean*, edited by B.N. Desai, pp. 271–284, A.A. Balkema, Brookfield, Vt., 1992

Cohen, Y., Consumption of dissolved nitrous oxide in an anoxic basin, Saanich Inlet, British Columbia, *Nature, 272*, 235–237, 1978.

Cohen, Y., and L.I. Gordon, Nitrous oxide production in the ocean, *J. Geophys Res., 84*, 347–353, 1979.

Desai, B.N. (Ed), *Oceanography of the Indian Ocean*, 780 pp., A.A Balkema, Brookfield, Vt., 1992

De Wilde, H.P.J., and W Helder, Nitrous oxide in the Somali Basin· The role of upwelling, *Deep Sea Res., Part II, 44*, 1319–1340, 1997

Dore, J.E., B.N. Popp, D.M Karl, and F J. Sansone, A large source of atmospheric nitrous oxide from subtropical North Pacific surface waters, *Nature*, *396*, 63–66, 1998.

Elkins, J W., Determination of dissolved nitrous oxide in aquatic systems by gas chromatography using electron capture detection and multi phase equilibration, *Anal Chem., 52*, 263–267, 1980.

Elkins, J.W., S C Wofsy, M.B. McElroy, C.E. Kolb, and W.A. Kaplan, Aquatic sources and sinks for nitrous oxide, *Nature, 275*, 602–606, 1978

Farrenkopf, A.M., G.W. Luther III, V.W. Truesdale, and C H. Van der Weijden, Sub-surface iodide maxima: Evidence for biologically catalyzed redox cycling in the Arabian Sea OMZ during the SW monsoon, *Deep Sea Res , Part II, 44*, 1391–1409, 1997.

Froelich, P.N., G P Klinkhammer, M.L. Bender, N.A. Luedtke, G R Heath, D Cullen, P. Dauphin, D. Hammond, B Hartman, and V Maynard, Early oxidation of organic matter in pelagic sediments of the eastern equatorial Atlantic· Suboxic diagenesis, *Geochim Cosmochim. Acta, 43*, 1075–1090, 1979.

Gage, J.D., L.A. Levin, and G.A. Wolff (Eds), Benthic processes in the deep Arabian Sea, *Deep Sea Res , Part II, 47*, 1–375, 2000

Hashimoto, L.K., W.A Kaplan, S.C. Wofsy, and M B McElroy, Transformation of fixed nitrogen and N_2O in the Cariaco Trench, *Deep Sea Res., Ser. A, 30*, 575–590, 1983.

Ittekkot, V., and R R. Nair (Eds.), *Monsoon Biogeochemistry*, 200 pp., Selbstverlag des Geol.-Paläontologischen Inst. der Univ Hamburg, Hamburg, Germany, 1993.

Khalil, M.A.K., and R.A. Rasmussen, The global sources of nitrous oxide, *J. Geophys. Res., 97*, 14,651–14,660, 1992.

Kim, K.-R., and H. Craig, Two-isotope characterization of N_2O in the Pacific Ocean and constraints on its origin in deep water, *Nature, 347*, 58–61, 1990.

Krishnaswami, S., and R.R. Nair (Eds.), Special Section: JGOFS (India), *Curr. Sci., 71*, 831–905, 1996.

Lal, D. (Ed), *Biogeochemistry of the Arabian Sea*, 250 pp., Indian Acad. of Sci., Bangalore, 1994.

Lal, S., P.K. Patra, S Venkataramani, and M.M. Sarin, Distribution of nitrous oxide and methane in the Arabian Sea, *Curr Sci., 71*, 894–899, 1996.

Law, C.S , and N.J.P. Owens, Significant flux of atmospheric nitrous oxide from the northwest Indian Ocean, *Nature, 346*, 826–828, 1990

Lee, C., et al., Particle organic carbon fluxes: Compilation of results from the 1995 US JGOFS Arabian Sea Process Study, *Deep Sea Res., Part II, 45*, 2489–2501, 1998.

Mantoura, R.F C , C.S. Law, N.J.P. Owens, P H. Burkill, E M S Woodward, R J.M. Howland, and C.A. Llewellyn, Nitrogen biogeochemical cycling in the northwestern Indian Ocean, *Deep Sea Res., Part II, 40*, 651–671, 1993.

McAllister, W.A , and W V Southerland, New use for a 0.5-nanometer molecular sieve gas chromatography column, *Anal Chem., 43*, 1536, 1971

Morrison, J.M., L.A Codispoti, S. Gaurin, B. Jones, V Manghnani, and Z. Zheng, Seasonal variation of hydrographic and nutrient fields during the US JGOFS Arabian Sea Process Study, *Deep Sea Res., Part II, 45*, 2053–2101, 1998.

Naqvi, S.W.A., Geographical extent of denitrification in the Arabian Sea, *Oceanol Acta, 14*, 281–290, 1991

Naqvi, S.W.A., Denitrification processes in the Arabian Sea, in *The Biogeochemistry of the Arabian Sea*, edited by D. Lal, pp. 181–202, Indian Acad. of Sci., Bangalore, 1994.

Naqvi, S.W.A., and R.J. Noronha, Nitrous oxide in the Arabian Sea, *Deep Sea Res., 38*, 871–890, 1991.

Naqvi, S.W.A., and M.S. Shailaja, Activity of the respiratory electron transport system and respiration rates within the oxygen minimum layer of the Arabian Sea, *Deep Sea Res., Part II, 40*, 687–695, 1993.

Naqvi, S.W.A., R.J. Noronha, M.S. Shailaja, K. Somasundar, and R. Sen Gupta, Some aspects of the nitrogen cycling in the Arabian Sea, in *Oceanography of the Indian Ocean*, edited by B N. Desai, pp. 285–311, A.A Balkema, Brookfield, Vt., 1992

Naqvi, S.W.A., D.A. Jayakumar, M. Nair, M.D. Kumar, and M.D. George, Nitrous oxide in the western Bay of Bengal, *Mar. Chem , 47*, 269–278, 1994.

Naqvi, S.W.A., T. Yoshinari, D A. Jayakumar, M.A.A Altabet, P.V Narvekar, A H. Devol, J.A. Brandes, and L.A. Codispoti, Budgetary and biogeochemical implications of N_2O isotope signatures in the Arabian Sea, *Nature, 394*, 462–464, 1998.

Nevison, C.D., R.F. Weiss, and D.J Erickson III, Global oceanic emissions of nitrous oxide, *J. Geophys Res., 100*, 15,809–15,820, 1995.

Olson, D.B , G.L Hitchcock, R.A. Fine, and B.A. Warren, Maintenance of the low-oxygen layer in the central Arabian Sea, *Deep Sea Res., Part II, 40*, 673–685, 1993.

Oudot, C , C Andrie, and Y. Montel, Nitrous oxide production in the tropical Atlantic Ocean, *Deep Sea Res., 37*, 183–202, 1990.

Patra, P.K., S. Lal, S. Venkataramani, S.N. De Sousa, V.V.S.S. Sarma, and S. Sardesai, Seasonal and spatial variability in N_2O distribution in the Arabian Sea, *Deep Sea Res., Part I, 46*, 529–543, 1999.

Pierotti, D., and R.A. Rasmussen, Nitrous oxide measurements in the eastern tropical Pacific Ocean, *Tellus, 32*, 56–72, 1980.

Prather, M., R. Derwent, D. Ehhalt, P. Fraser, E. Sanhueza, and X. Zhou, Other trace gases and atmospheric chemistry, in *Climate Change 1995, The Science of Climate Change, Contribution of Working Group I to the Second Assessment of the Intergovernmental Panel on Climate Change*, edited by J T. Houghton et al , pp. 86–103, Cambridge Univ. Press, New York, 1996.

Rao, T.S.S., and R.C. Griffiths, *Understanding the Indian Ocean, Perspectives on oceanography*, 187 pp., United Nations Educ., Sci. and Cult. Org (UNESCO), Paris, 1998.

Rhein, M., L Stramma, and O. Plähn, Tracer signals of the intermediate layer of the Arabian Sea, *Geophys. Res. Lett., 24*, 2561–2564, 1997.

Rönner, U., Distribution, production and consumption of nitrous oxide in the Baltic Sea, *Geochim. Cosmochim. Acta, 47*, 2179–2188, 1983.

Schott, F.A., J. Fischer, U. Garternicht, and D. Quadfasel, Summer monsoon response of the northern Somali Current, 1995, *Geophys. Res. Lett , 24*, 2565-2568, 1997.

Shenoi, S S C., S.R Shetye, A.D. Gouveia, and G.S Michael, Salinity extrema in the Arabian Sea, in *Monsoon Biogeochemistry*, edited by V Ittekkot and R.R. Nair, pp. 37–49, Selbstverlag des Geol.-Paläontologischen Inst. der Univ. Hamburg, Hamburg, Germany, 1993.

Siedler, G., and H. Peters, Properties of sea water, in *Landolt–Börnstein, Oceanography, New Ser., Group V*, vol 3a, edited by J. Sündermann, pp. 233–264, Springer Verlag, New York, 1986.

Smith, S L. (Ed.), The 1994-1996 Arabian Sea expedition: Oceanic response to monsoonal forcing, Part 1, *Deep Sea Res , Part II, 45*, 1905–2501, 1998.

Smith, S.L (Ed.), The 1994-1996 Arabian Sea expedition: Oceanic response to monsoonal forcing, Part 2, *Deep Sea Res., Part II, 46*, 1531–1964, 1999.

Stumm, W., and J.J Morgan, *Aquatic Chemistry*, 1022 pp., John Wiley, New York, 1996.

Upstill-Goddard, R.C., J. Barnes, and N.J.P. Owens, Nitrous oxide and methane during the 1994 SW monsoon in the Arabian Sea/northwestern Indian Ocean, *J. Geophys. Res., 104*, 30,067–30,084, 1999.

Van Weering, T.C.E., W. Helder, and P. Schalk (Eds.), Netherlands Indian Ocean Program 1992–1993: First results, *Deep Sea Res., Part II, 44*, 1177–1480, 1997.

Weiss, R.F., The solubility of nitrogen, oxygen and argon in water and seawater, *Deep Sea Res., 17*, 721–735, 1970.

Weiss, R.F., and B.A Price, Nitrous oxide solubility in water and seawater, *Mar. Chem., 8*, 347–359, 1980.

Yoshida, N , H. Morimoto, M. Hirano, I. Koike, S Matsuo, E. Wada, T. Saino, and A Hattori, Nitrification rates and ^{15}N abundances of N_2O and NO_3^- in the western North Pacific, *Nature, 342*, 895–897, 1989.

Yoshinari, T., Nitrous oxide in the sea, *Mar. Chem., 4*, 189–202, 1976.

You, Y., Seasonal variations of thermocline circulation and ventilation in the Indian Ocean, *J. Geophys. Res., 102*, 10,391–10,422, 1997.

M. O. Andreae and H. W. Bange, Biogeochemistry Department, Max Planck Institute for Chemistry, P.O. Box 3060, D-55020 Mainz, Germany. (bange@mpch-mainz.mpg.de)

S. Rapsomanikis, Laboratory of Atmospheric Pollution Science and Technology, Environmental Engineering Department, Demokritos University of Thrace, GR-67100 Xanthi, Greece.

(Received May 19, 1999; revised August 1, 2000;
accepted August 23, 2000.)